HOKKAIDO UNIVERSITY

Title	Luminescence Changeable CO2-Storage Cylinder: Triple-Stranded Helical Eu(III)/Tb(III) Fluorinated MOFs with Amide Linkers
Author(s)	Hayashi, Joe; Iwamura, Shinichiro; Nakasaka, Yuta et al.
Citation	Chemistry-A European journal, 30(66), e202403224 https://doi.org/10.1002/chem.202403224
Issue Date	2024-11-26
Doc URL	https://hdl.handle.net/2115/95935
Rights	This is the peer reviewed version of the following article: J. Hayashi, S. Iwamura, Y. Nakasaka, M. Wang, S. Shoji, Y. Kitagawa, K. Fushimi, S. R. Mukai, Y. Hasegawa, Chem. Eur. J. 2024, 30, e202403224, which has been published in final form at https://doi.org/10.1002/chem.202403224. This article may be used for non-commercial purposes in accordance with Wiley Terms and Conditions for Use of Self-Archived Versions. This article may not be enhanced, enriched or otherwise transformed into a derivative work, without express permission from Wiley or by statutory rights under applicable legislation. Copyright notices must not be removed, obscured or modified. The article must be linked to Wiley's version of record on Wiley Online Library and any embedding, framing or otherwise making available the article or pages thereof by third parties from platforms, services and websites other than Wiley Online Library must be prohibited.
Type	journal article
File Information	Chem.-Eur. J.202403224.pdf

Hokkaido University Collection of Scholarly and Academic Papers : HUSCAP

RESEARCH ARTICLE

Luminescence changeable CO_2-storage cylinder: Triple-stranded helical Eu(III)/Tb(III) fluorinated MOFs with amide linkers

Joe Hayashi,[a] Shinichiro Iwamura,[b] Yuta Nakasaka,[c] Mengfei Wang,[c,d] Sunao Shoji,[e] Yuichi Kitagawa,[c] Koji Fushimi,[c] Shin R. Mukai,[c] Yasuchika Hasegawa*[c,d]

[a] J. Hayashi
Graduate School of Chemical Sciences and Engineering
Hokkaido University
Kita 13 Nishi 8 Kita-ku, Sapporo, Hokkaido 060-8628 (Japan)
[b] S. Iwamura
Advanced Institute for Materials Research (WPI-AIMR)
Tohoku University
2-1-1 Katahira Aoba-ku, Sendai, Miyagi 980-8577 (Japan)
[c] Y. Nakasaka, M. Wang, Y. Kitagawa, K. Fushimi, S. Mukai, Y. Hasegawa
Faculty of Engineering, Hokkaido University
Kita 13 Nishi 8 Kita-ku, Sapporo, Hokkaido 060-8628 (Japan)
E-mail: hasegaway@eng.hokudai.ac.jp
[d] M. Wang, Y. Hasegawa
Institute for Chemical Reaction Design and Discovery (WPI-ICReDD)
Hokkaido University
Kita 21 Nishi 10 Kita-ku, Sapporo, Hokkaido 001-0021 (Japan)
[e] S. Shoji
Faculty of Engineering
Nara Women's University
Kitauoya-Nishimachi, Nara 630-8506 (Japan)

Supporting information for this article is given via a link at the end of the document.

Abstract: Triple-stranded helical lanthanide MOFs with CO_2 adsorption properties were investigated. Lanthanide MOFs ($[Eu_{0.1}Tb_{0.9}(hfa)_3(dpa)]_n$) are composed of lanthanide luminophores (Eu(III) and/or Tb(III) ions), fluorinated antenna ligands (hfa: hexafluoroacetylacetonate), and polyamide-type linker ligands (dpa: 4-(diphenylphosphoryl)-*N*-(4-(diphenylphosphoryl)phenyl)benzamide). The cylindrical structure was characterized by single-crystal X-ray analysis, thermogravimetric analysis, and gas adsorption measurements. The inner surfaces of the cylindrical channels were covered with the fluorine atoms of the hfa ligands. The emission intensity ratio (I_{Eu} / I_{Tb}) in $[Eu_{0.1}Tb_{0.9}(hfa)_3(dpa)]_n$ is affected by the CO_2 gas adsorption behavior. The change in I_{Eu} / I_{Tb} value was caused by the intermolecular interactions between the CO_2 gas molecules and the fluorinated ligands, resulting in an electronic structural change of the lowest triplet excited state in the photosensitized hfa ligands.

Introduction

Effective CO_2 gas capture from air is now the focus of modern environmental and industrial chemistry.[1-3] Metal-organic frameworks (MOFs) are promising materials for CO_2 gas capture.[4,5] Compared with inorganic compounds such as zeolites and mesoporous silica, the characteristic structure of MOFs involves adjustable pore sizes and functional modifications.[6,7]

CO_2 gas capture using luminescent MOF materials is desirable for visualization of the captured gas. Yanai reported a Zn-MOF that encapsulated luminescent distyrylbenzene.[8] Their fluorescence response is caused by the structural transformation of the MOFs, including distyrylbenzene, during CO_2 adsorption. Das described Cr/Al-MOFs with luminescent amidine groups that exhibited high CO_2 selectivity using a fluorescence quenching mechanism.[9]

In this paper, we report a luminescent porous Eu(III)/Tb(III)-mixed MOF to visualize CO_2 gas capture. The Eu(III) and Tb(III) ions exhibited 4f-4f transition-based red and green emissions, respectively. We previously reported a ratiometric temperature sensor using Eu(III)/Tb(III)-mixed MOFs.[10] Ratiometric analysis of two lanthanide luminophores is a potential method for sensing applications. In this study, CO_2 detection was achieved using a Eu(III)/Tb(III) ratiometric analysis system.

Herein, we demonstrate the design of a lanthanide MOFs with an inner channel for CO_2 detection. We focused on a helical cylindrical structure to construct an inner channel for CO_2 gas adsorption. A flexible V-shaped amide spacer has been reported for the successful construction of helical coordination structure.[11-14] Amide linker ligand **dpa** (4-(diphenylphosphoryl)-N-(4-(diphenylphosphoryl)phenyl)benzamilde) was selected for the cylindrical structure. Additionally, to create strong binding interactions with the electropositive carbon atom of the CO_2 molecule,[15,16] **hfa** ligand (hexafluoroacetylacetonate) accompanied by electronegative fluorine atoms was chosen. In contrast, hfa-coordinated red Eu(III) and green Tb(III) luminophores were utilized to achieve ratiometric emission (I_{Eu} / I_{Tb}) for observing CO_2 adsorption. Therefore, a luminescent Eu(III)/Tb(III)-mixed MOFs with a helical cylindrical structure was prepared (Figure 1). The structural design of the MOFs i) produces a highly ordered helical structure, ii) positions the fluorinated units on the inner surface of the helical cylinder, facilitating CO_2 storage, and iii) enables ratiometric detection by monitoring the Eu(III)/Tb(III) emission intensity. In addition, a Gd(III) MOF was prepared to estimate the excited triplet lifetime

of the **hfa** ligands under CO_2 gas condition. As a reference, we prepared two lanthanide coordination polymers, **[Eu(hfa)$_3$(*p*-dpba)]$_n$** and **[Eu(acac)$_3$(dpba)]$_n$** (Figure 1; *p*-dpba: *N*,*N*'-(1,4-phenylene)bis(4-(diphenylphosphoryl)benzamide), acac: acetylacetonate). **[Eu(hfa)$_3$(*p*-dpba)]$_n$**. has double amide linker ligand. We also lanthanide coordination polymer with non-fluorinated ligand, **[Eu(acac)$_3$(dpba)]$_n$**. This study demonstrates a luminescence changeable CO_2-storage cylinder composed of a triple-stranded helical Eu(III)/Tb(III) MOF, **[Eu$_{0.1}$Tb$_{0.9}$(hfa)$_3$(dpba)]$_n$**.

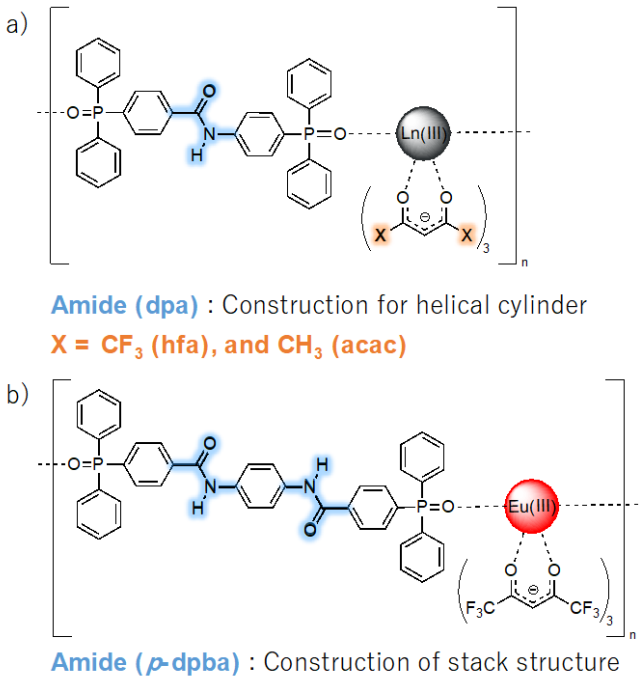


Figure 1. a) Molecular structure of **[Ln(hfa)$_3$(dpa)]$_n$ (Ln = Eu, Tb, and Gd)** and **[Eu(acac)$_3$(dpba)]$_n$**. b) Molecular structure of **[Eu(hfa)$_3$(*p*-dpba)]$_n$**.

Results and Discussion

The lanthanide MOFs, **[Eu(hfa)$_3$(dpa)]$_n$**, **[Tb(hfa)$_3$(dpa)]$_n$**, **[Gd(hfa)$_3$(dpa)]$_n$**, and **[Eu$_{0.1}$Tb$_{0.9}$(hfa)$_3$(dpa)]$_n$** were obtained by the reaction of **(dpa)** with precursor complex, [Ln(hfa)$_3$(H$_2$O)$_2$] (Ln = Eu, Tb, and Gd), in methanol under reflux condition (Schemes S1 and S2). Single crystals of lanthanide MOFs were obtained by the recrystallization from a methanol/acetonitrile mixture solution. The crystal structure of **[Eu(hfa)$_3$(dpa)]$_n$** is shown in Figure 2a. The crystallographic data presented in Table S1. The Eu(III) ions were coordinated to eight oxygen atoms from three **hfa** ligands and two **dpa** ligands. Based on their crystal data, we performed continuous shape measure (CShM) calculations using SHAPE to determine the geometrical structures around the Eu(III) ions in the first coordination sphere (see SI).[17, 18] The geometrical symmetry around the Eu(III) ions was determined to be an 8-coordinated square-antiprismatic structure (point group = D_{4d}). The two phosphine oxide groups in the **dpa** ligand were attached to different Eu(III) ions to form a triple-stranded helical structure. The helical structure provided cylindrical channels along the c-axis (Figure 2b and 2c). The inner surfaces of the channels were covered with the F atoms of the **hfa** units. The diameter of the

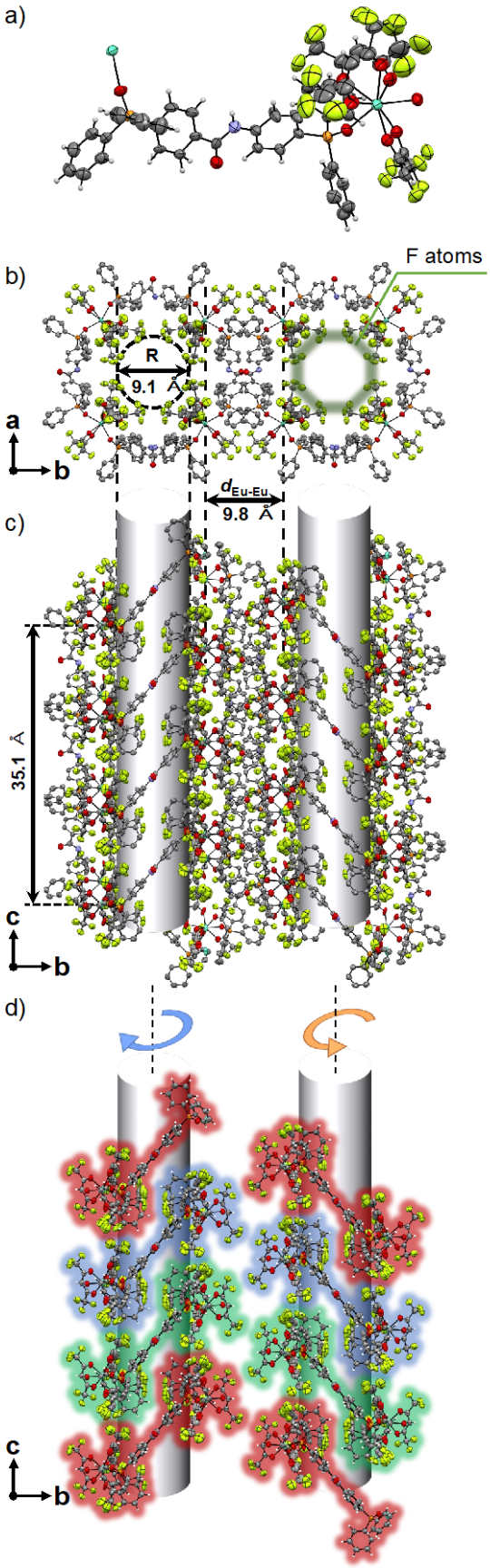


Figure 2. a) ORTEP drawings (ellipsoids set at 50 % probability, hydrogen atoms were omitted for clarity) of **[Eu(hfa)$_3$(dpa)]$_n$**. Views of **[Eu(hfa)$_3$(dpa)]$_n$** b) along c axis and c) along a axis. d) View of the left- and right-handed helical chains in **[Eu(hfa)$_3$(dpa)]$_n$**.

channel is estimated to be 9.1 Å, which is larger than that of the CO_2 molecule (3.4 Å). The Eu-Eu distance between the cylindrical channels (d_{Eu-Eu}) was 9.8 Å. The pitch of the helical chains was 35.1 Å. The three polymer chains form a triple-stranded helical structure (Figure 2d). Their right-handed and left-handed helical chains are arranged, alternately. The powder X-ray diffraction (PXRD) pattern of **[Eu(hfa)$_3$(dpa)]$_n$** matched with the simulated pattern of the single-crystal structure (Figure S1a). The PXRD patterns of **[Tb(hfa)$_3$(dpa)]$_n$**, **[Gd(hfa)$_3$(dpa)]$_n$**, and **[Eu$_{0.1}$Tb$_{0.9}$(hfa)$_3$(dpa)]$_n$** were similar to those of **[Eu(hfa)$_3$(dpa)]$_n$** (Figure S1a). The decomposition temperature of **[Eu(hfa)$_3$(dpa)]$_n$** was found to be around 320 °C from the TGA profile (Figure S2). The crystal structure of **[Eu(hfa)$_3$(*p*-dpba)]$_n$** is shown in Figure 3a. The crystallographic data presented in Table S1. The Eu(III) ions of **[Eu(hfa)$_3$(*p*-dpba)]$_n$** were also coordinated to eight oxygen atoms from three **hfa** ligands and two ***p*-dpba** ligands. The geometrical symmetry around the Eu(III) ions was determined to be an 8-coordinated square-antiprismatic structure (point group = D_{4d}). The two phosphine oxide groups in the ***p*-dpba** ligand were attached to different Eu(III) ions to form stacking structure without inner channel (Figure 3b). The PXRD measurement for **[Eu(acac)$_3$(dpa)]$_n$** were performed (Figure S1b). The characteristic peaks were observed.

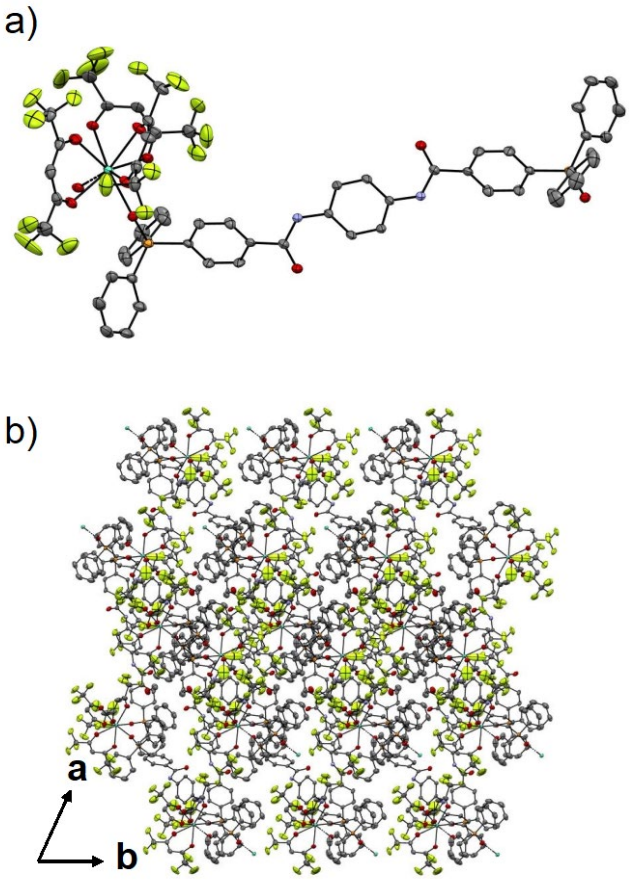


Figure 3. a) ORTEP drawings (ellipsoids set at 50 % probability, hydrogen atoms were omitted for clarity) of **[Eu(hfa)$_3$(*p*-dpba)]$_n$**. b) Views of **[Eu(hfa)$_3$(*p*-dpba)]$_n$** along c axis.

The gas adsorption capacity of **[Eu(hfa)$_3$(dpa)]$_n$** was estimated from the CO_2 and N_2 adsorption isotherms at 298 K (Figure 4). In the CO_2 adsorption measurements, we observed a characteristic linear plot of the gas adsorption isotherms. However, adsorption of N_2 gas was not observed. The reversibility between gas adsorption and desorption behavior was indicated. The CO_2 gas adsorption and desorption behaviors of **[Eu(hfa)$_3$(*p*-dpba)]$_n$** and **[Eu(acac)$_3$(dpa)]$_n$** was not observed (Figure 4). The selectivity of CO_2 adsorption is due to its quadrupole moment, which results in a stronger interaction with the CF_3 groups on the inner surface of the cylindrical channels.[19]

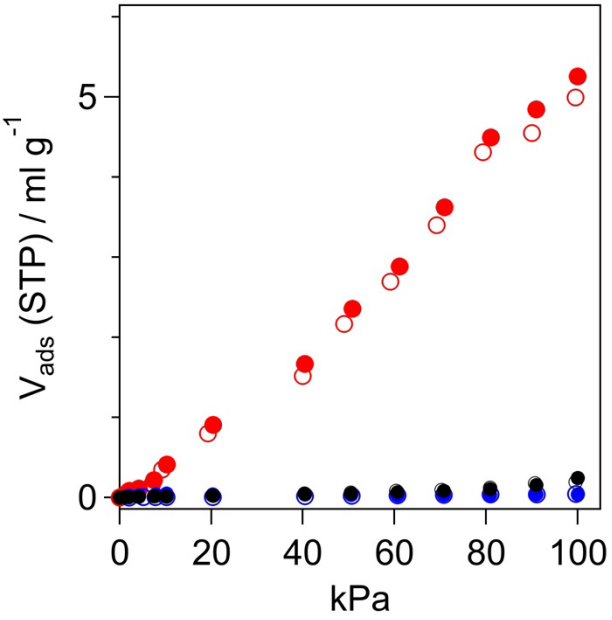


Figure 4. CO_2 adsorption (solid symbols) and desorption (open symbols) isotherms of a) **[Eu(hfa)$_3$(dpa)]$_n$** (red), **[Eu(hfa)$_3$(*p*-dpba)]$_n$** (blue) and **[Eu(acac)$_3$(dpa)]$_n$** (black) at 298 K.

The excitation and emission spectra of **[Eu(hfa)$_3$(dpa)]$_n$** was are shown in Figure S3a. The emission bands at 578, 590, 610, 652, and 700 nm are assigned to be $^5D_0 \rightarrow {}^7F_0$, $^5D_0 \rightarrow {}^7F_1$, $^5D_0 \rightarrow {}^7F_2$, $^5D_0 \rightarrow {}^7F_3$, and $^5D_0 \rightarrow {}^7F_4$ transitions of Eu(III), respectively (Figure S3a).[20] The excitation bands observed in the UV region were attributed to the π–π^* transition of **hfa** ligand. The shape emission spectra of **[Eu(hfa)$_3$(dpa)]$_n$** are also measured in CO_2 and N_2 condition (Figure S4a). The time-resolved luminescence decay profiles obtained the emission lifetimes (τ_{obs}). The τ_{obs} under CO_2 condition was estimated to be 0.81 ms, which is the same as that under N_2 gas (Table 1). Photophysical parameters were calculated based on the emission spectra and lifetime, photophysical parameters were calculated (Table S2). The overall emission quantum yield (excited at π–π^* transition band of **hfa** ligands, $\Phi_{\pi\pi*}$) under each condition was around 61% (Table 1). **[Tb(hfa)$_3$(dpa)]$_n$** also showed excitation bands in the UV region and emission bands at 490, 540, 580, 620, and 650 nm, corresponding to $^5D_4 \rightarrow {}^7F_6$, $^5D_4 \rightarrow {}^7F_5$, $^5D_4 \rightarrow {}^7F_4$, $^5D_4 \rightarrow {}^7F_3$, and $^5D_4 \rightarrow {}^7F_2$ transitions of Tb(III), respectively (Figure S3b). The similar shape of **[Tb(hfa)$_3$(dpa)]$_n$** emission spectra are also measured in CO_2 and N_2 condition (Figure S4b). The emission

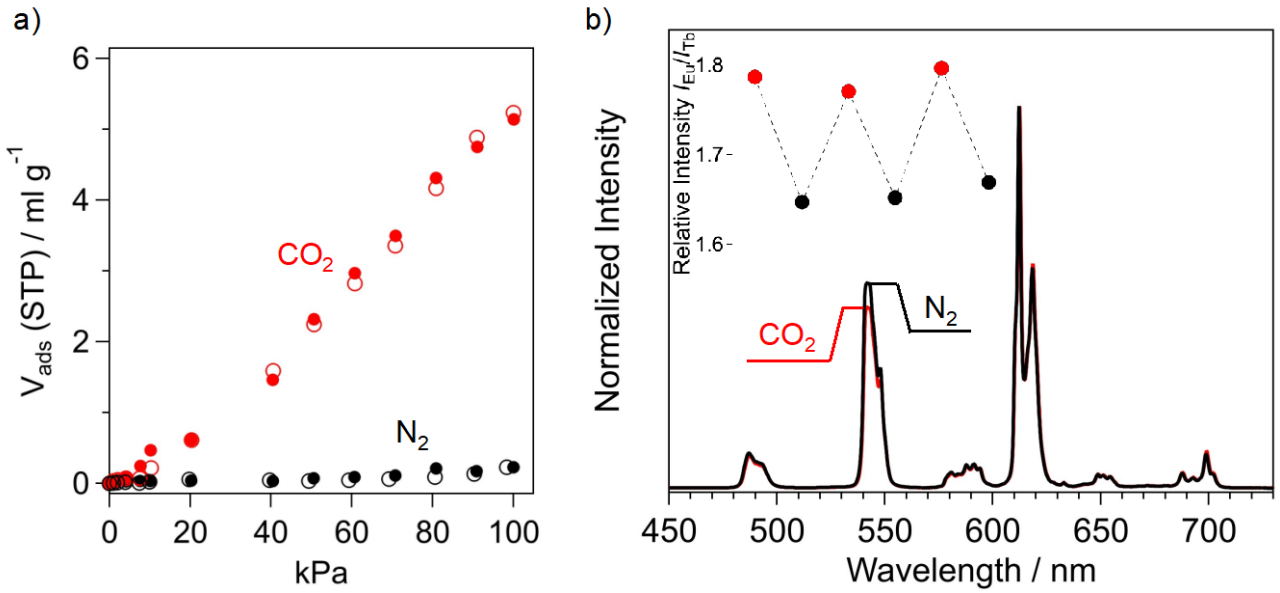


Figure 5. a) CO_2 (red) and N_2 (black) adsorption (solid symbols) and desorption (open symbols) isotherms of **[Eu$_{0.1}$Tb$_{0.9}$(hfa)$_3$(dpa)]$_n$** at 298 K. b) Normalized emission spectra of **[Eu$_{0.1}$Tb$_{0.9}$(hfa)$_3$(dpa)]$_n$** under CO_2 (red) and N_2 (black) condition (λ_{ex} = 370 nm). Recycle measurement of emission intensity ratio between Eu and Tb in **[Eu$_{0.1}$Tb$_{0.9}$(hfa)$_3$dpa]$_n$** (inset).

quantum yields of **[Tb(hfa)$_3$(dpa)]$_n$** were 9.5% (under CO_2) and 11.6% (under N_2) (Table 1). The τ_{obs} was estimated to be 0.13 ms (under CO_2) and 0.14 ms (under N_2) (Table 1).

Table 1. Photophysical parameters of lanthanide MOFs.

Compound	Gas	τ_{obs} / ms	$\Phi_{\pi\pi^*}$ / %[c]	I_{Eu} / I_{Tb}[c]
[Eu(hfa)$_3$(dpa)]$_n$	CO_2	0.81[a]	61.3	--
	N_2	0.81[a]	61.1	--
[Tb(hfa)$_3$(dpa)]$_n$	CO_2	0.13[b]	9.5	--
	N_2	0.14[b]	11.6	--
[Eu$_{0.1}$Tb$_{0.9}$(hfa)$_3$(dpa)]$_n$	CO_2	0.13[b]	20.8	1.9
	N_2	0.16[b]	24.6	1.8

[a] λ_{ex} = 355 nm, λ_{em} = 610 nm. [b] λ_{ex} = 355 nm, λ_{em} = 540 nm, [c] λ_{ex} = 370 nm.

The emission spectra of **[Eu$_{0.1}$Tb$_{0.9}$(hfa)$_3$(dpa)]$_n$** in CO_2 and N_2 condition are shown in Figure 5b. The emission intensity ratio between Tb(III) (corresponding to 542 nm) and Eu(III) (corresponding to 612 nm), denoted as I_{Eu} / I_{Tb}, depends on the gas condition. The calculated I_{Eu} / I_{Tb} values were calculated to be 1.9 (under CO_2) and 1.8 (under N_2), respectively (Table 1). Photographs of the emission of **[Eu$_{0.1}$Tb$_{0.9}$(hfa)$_3$dpa]$_n$** under N_2 and CO_2 condition are shown in Figure S5. We cannot observe the drastic change of emission color between N_2 and CO_2 condition. On the other hand, recycling emission spectra between CO_2 and N_2 was investigated for **[Eu$_{0.1}$Tb$_{0.9}$(hfa)$_3$dpa]$_n$** (Figure 5b, inset). The coordination polymer exhibited reversible intensity ratio between Eu(III) and Tb(III). The CO_2 gas caused the change in I_{Eu} / I_{Tb} value. CO_2 gas adsorption promoted a lifetime change in the excited triplet state of the photosensitized **hfa** ligand. Previously, we reported that the excited-state equilibrium between the $^5D_4$ (Tb) and T_1 (**hfa**) states affected the change in emission lifetime.[21] From the viewpoint of the emission lifetime in the excited triplet state, the emission lifetimes of **[Gd(hfa)$_3$(dpa)]$_n$** under CO_2 and N_2 conditions were measured (Table S3). The emission lifetime in the CO_2 condition (τ = 0.36 ms) was shorter than in the N_2 condition (τ = 0.38 ms).

The τ_{obs} of **[Eu$_{0.1}$Tb$_{0.9}$(hfa)$_3$(dpa)]$_n$** was estimated to be 0.13 ms (under CO_2) and 0.16 ms (under N_2) (Table 1). The τ_{obs} under degas condition were measured to be 0.15 ms. The pressure sensitivity was calculated to be 0.20 μs kPa^{-1}. This value is almost same as previously reported optical membrane sensor with Ru(II) (0.23 μs kPa^{-1}). The lifetime of **[Eu$_{0.1}$Tb$_{0.9}$(hfa)$_3$dpa]$_n$** is similar to that of previous optical Ru(II) membrane sensor.[22]

Conclusion

In conclusion, novel MOFs formed by triple-stranded helical lanthanide polymers were successfully synthesized. The characteristic cylindrical structure of the triple-stranded helical MOF facilitated CO_2 adsorption behavior. The F atoms of the **hfa** unit on the inner surface of the cylinder promote CO_2 gas adsorption properties, although the image of CO_2 fixation with Eu/Tb helical structure was not obtained at the present stage. Lanthanide MOFs are promising materials for the selective adsorption, visualization, and separation of CO_2 from industrial fuel gases. We are now attempting to conduct more precise and quantitative experiments to gain further insight into gas storage.

Experimental Section

General methods: ^{1}H, ^{13}C, and ^{31}P NMR spectra were recorded on a JEOL ECS400 and ECZ400S. Tetramethylsilane (δ_H = 0.00 ppm) and phosphoric acid (δ_P = 0.00 ppm) were used as references for ^{1}H and ^{31}P NMR, respectively. ESI-MS spectra were measured using a JEOL JMS-T100LP. Elemental analysis was performed using MICRO CORDER JM10 and Exeter Analytical CE440 instrument. Powder X-ray diffraction was performed on a Rigaku SmartLab (CuKα radiation, λ = 1.5418 Å) Excitation and emission spectra under air condition were measured using a HORIBA Fluorolog-3 spectrofluorometer. Emission spectra under CO_2 and N_2 gas condition were measured using a HORIBA Fluorolog-3 spectrofluorometer with a cryostat (Thermal Block Company SA-SB245T). Emission lifetimes (τ_{obs}) were measured using the third harmonics (355 nm) of a Q-switched Nd:YAG laser (Spectra Physics, INDI-50, FWHM = 5 ns, λ = 1064 nm) and a photomultiplier (Hamamatsu photonics, R5108, response time ≤ 1.1 ns). The Nd:YAG laser response was monitored using a digital oscilloscope (TDS3052, 500 MHz, Sony Tektronix) synchronized to the single-pulse excitation. The emission lifetimes were determined from the slopes of the logarithmic plots of the decay profiles. The emission quantum yields ($\Phi_{\pi\pi^*}$) were estimated using a JASCO F-6300-H spectrometer attached to a JASCO ILF-533 integrating sphere unit (Φ = 100 mm). Gas adsorption measurement was recorded on a BELSORP MAX (MicrotracBeL Corp.).

Materials: Europium acetate n-hydrate (99.9%), terbium(III) acetate tetrahydrate (99.9%), and gadolinium(III) acetate tetrahydrate (99.9%) were obtained from FUJIFILM Wako Pure Chemical Corporation. All other reagents were of reagent grade were used without further purification.

Preparation of 4-(diphenylphosphinyl)benzenamine (1): Potassium acetate (176.7 mg, 1.8 mmol), 4-iodoaniline (328.5 mg, 1.5 mmol), palladium(II) acetate (0.34 mg, 1.5 μmol) were dissolved in DMA (10 ml) at room temperature under Ar atmosphere. After diphenyl phosphine (0.29 ml, 1.5 mmol) was added to the solution, the solution was stirred at 130°C for 3 h. The reaction mixture was cooled to room temperature and the solvent was evaporated in vacuo. The residue was dissolved in CH_2Cl_2 and washed with aqueous 5% $NaHCO_3$ and distilled water. The organic layer was concentrated in vacuo. The residue was dissolved in CH_2Cl_2 (10 ml) and added aqueous 30% H_2O_2 (1 ml) at 0°C. After stirring for 1 h, the reaction mixture was washed with distilled water. The organic layer was dried over Na_2SO_4 and evaporated to give **1** (154.3 mg, 0.526 mmol, 35.0%) as a white solid: ^{1}H NMR (400 MHz, $CDCl_3$) δ 7.69–7.64 (4H, m), 7.54–7.50 (2H, m), 7.46–7.36 (6H, m), 6.69–6.66 (2H, m), 4.09 (2H, s) ppm. ^{13}C NMR (100 MHz, $CDCl_3$) δ 149.9, 149.9, 133.8, 133.7, 132.8, 132.1, 132.0, 131.6, 131.6, 128.4, 128.3, 120.3, 119.2, 114.3, 114.2 ppm. ^{31}P NMR (162 MHz, $CDCl_3$) δ 29.7 ppm. MS(ESI) found: m/z 316.09. Calcd. for $C_{18}H_{16}NNaOP$: $[M+Na]^+$, 316.09.

Preparation of 4-(diphenylphosphoryl)benzoic acid (2) : 4-(diphenylphosphoryl)benzoic acid **2** was synthesized according to the previously reported procedures.[23]

Preparation of dpa: Thionyl chloride (1 ml) was added to compound 2 (322.3 mg, 1 mmol) at room temperature. After stirring for 30 min, the reaction mixture was concentrated in vacuo. The resulting residue was dissolved in CH_2Cl_2 (10 ml). Compound 1 (293.3 mg, 1 mmol) and Et_3N (0.3 ml) were added to the solution. After stirring for 2 h at room temperature, the reaction mixture was washed with aqueous 2% HCl, aqueous 5% $NaHCO_3$, and distilled water. The organic layer was dried over Na_2SO_4 and evaporated. The residue was purified by silica gel column chromatography (5% MeOH–CH_2Cl_2) to give **dpa** (299.0 mg, 0.500 mmol, 50.0%) as white solid: ^{1}H NMR (400 MHz, $CDCl_3$) δ 10.89 (1H, s), 8.03–8.00 (4H, m), 7.67–7.40 (24H, m) ppm. ^{13}C NMR (101 MHz, $CDCl_3$) δ 166.2, 142.6, 138.7, 135.5, 134.5, 132.9, 132.8, 132.7, 132.3, 132.3, 132.0, 132.0, 131.9, 131.9, 131.8, 131.8, 131.7, 130.8, 128.7, 128.6, 128.5, 128.4, 128.1, 128.0, 127.1, 126.0, 120.4, 120.3 ppm. ^{31}P NMR (162 MHz, $CDCl_3$) δ 29.5, 29.2 ppm. MS(ESI) found: m/z 620.15. Calcd. for $C_{37}H_{29}NNaO_3P_2$: $[M+Na]^+$, 620.15.

Preparation of $[Ln(hfa)_3(H_2O)_2]$ (Ln = Eu, Tb, and Gd): $[Ln(hfa)_3(H_2O)_2]$ was synthesized according to the previously reported procedures.[24, 25, 26]

Preparation of $[Ln(hfa)_3(dpa)]_n$ (Ln = Eu, Tb, and Gd): $[Ln(hfa)_3(H_2O)_2]$ (0.1 mmol) was added to a MeOH (10 ml) solution of dpa (59.8 mg, 0.1 mmol), and the mixture was refluxed for 1 h. The recrystallization from acetonitrile and MeOH gave **$[Ln(hfa)_3(dpa)]_n$** as a white powder.

$[Eu(hfa)_3(dpa)]_n$: yield 46.3%. MS(ESI) found: m/z 1394.04. Calcd. for $C_{52}H_{32}EuF_{18}NNaO_9P_2$: $[M+Na]^+$, 1394.04. Elemental analysis: found (%): C 45.47, H 2.30, N 1.15. Calcd. for $C_{52}H_{32}EuF_{18}NO_9P_2$: C 45.57, H 2.35, N 1.02.

$[Tb(hfa)_3(dpa)]_n$: yield 43.9%. MS(ESI) found: m/z 1400.05. Calcd. for $C_{52}H_{32}F_{18}NNaO_9P_2Tb$: $[M+Na]^+$, 1400.04. Elemental analysis: found (%): C 45.29, H 2.37, N 1.10. Calcd. for $C_{52}H_{32}F_{18}NNaO_9P_2Tb$: C 45.34, H 2.34, N 1.02.

$[Gd(hfa)_3(dpa)]_n$: yield 45.5%. MS(ESI) found: m/z 1399.04. Calcd. for $C_{52}H_{32}F_{18}GdNNaO_9P_2$: $[M+Na]^+$, 1399.09. Elemental analysis: found (%): C 45.67, H 2.38, N 1.12. Calcd. for $C_{52}H_{32}F_{18}GdNO_9P_2$: C 45.39, H 2.34, N, 1.02.

Preparation of $[Eu_{0.1}Tb_{0.9}(hfa)_3(dpa)]_n$: $[Eu(hfa)_3(H_2O)_2]$ (8.09 mg, 0.01 mmol) and $[Tb(hfa)_3(H_2O)_2]$ (53.9 mg, 0.09 mmol) was added to a MeOH (10 ml) solution of **dpa** (59.8 mg, 0.1 mmol), and the mixture was refluxed for 1 h. The recrystallization from acetonitrile and MeOH gave the corresponding europium/terbium mixed MOF **$[Eu_{0.1}Tb_{0.9}(hfa)_3(dpa)]_n$** (57.7 mg, 41.9 μmol, 41.9%) as a white powder: Elemental analysis: found (%): C 45.51, H 2.50, N,1.26. Calcd. for $C_{52}H_{32}Eu_{0.1}F_{18}NO_9P_2Tb_{0.9}$: C 45.36, H 2.34, N 1.02.

Preparation of *p*-dpba (5): 4-(diphenylphosphoryl)benzoic acid **2** (322.3 mg, 1.0 mmol) was dissolved in thionyl chloride (1 mL) and stirred for 30 min at room temperature. The solvent was

removed in vacuo. The residue was dissolved in dichloromethane (10 mL), and successively added *p*-phenylenediamine (54.07 mg, 0.5 mmol) and triethylamine (1 mL) at 0°C. After stirring for 2 hours at room temperature, the reaction mixture was filtered. The precipitation was purified by recrystallization from dichloromethane and MeOH to give **5** (158.4 mg, 0.221 mmol, 44.2%): ^{1}H NMR (400 MHz, DMSO-d_6) δ 10.37 (2H, s), 8.07 (4H, d), 7.80-7.56 (34H, m) ppm. ^{13}C NMR (100 MHz, DMSO-d_6) δ 164.7, 138.2, 136.3, 135.3, 134.9, 132.8, 132.2, 131.7, 131.6, 131.5, 131.4, 128.9, 128.8, 127.8, 127.7, 120.7 ppm. ^{31}P NMR (162 MHz, DMSO-d_6) δ 25.8 ppm. MS(ESI) found: m/z 739.19. Calcd. for $C_{44}H_{34}N_2NaO_4P_2$: $[M+Na]^+$, 739.19.

Preparation of [Eu(hfa)$_3$(*p*-dpba)]$_n$: [Eu(hfa)$_3$(H_2O)$_2$] (80.9 mg, 0.1 mmol) was added to a dichloromethane (5 ml) and MeOH (5 ml) mixture solution of ***p*-dpba** (71.6 mg, 0.1 mmol), and the mixture was stirred for 1 h. The recrystallization from dichloromethane and gave **[Eu(hfa)$_3$(*p*-dpba)]$_n$** (39.0 mg, 26.2 μmol, 26.2%) as a white powder: MS(ESI) found: m/z 1513.09. Calcd. for $C_{59}H_{37}EuF_{18}N_2NaO_{10}P_2$: $[M+Na]^+$, 1513.07.

Preparation of [Eu(acac)$_3$(dpa)]$_n$: [Eu(acac)$_3$·nH_2O] (44.2 mg, 0.1 mmol) was added to a MeOH (10 ml) mixture solution of **dpa** (59.8 mg, 0.1 mmol), and the mixture was refluxed for 1 h. The reaction mixture was evaporated to give **[Eu(acac)$_3$(dpa)]$_n$** (31.8 mg, 30.4 μmol, 30.4%) as a white powder: MS(ESI) found: m/z 1070.20. Calcd. for $C_{52}H_{50}EuNNaO_9P_2$: $[M+Na]^+$, 1070.20.

Single-crystal X-ray structure determination: Single-crystal X-ray structural analyses were carried out using a Rigaku XtaLAB Synergy-R/DW equipped with a HyPix-6000HE detector (MoKα radiation, λ = 0.71073 Å). The structure was resolved using direct methods and expanded using Fourier transform techniques. The non-hydrogen atoms were refined anisotropically using the SHELX system.[27] Hydrogen atoms were refined using a riding model. All calculations were performed using the Olex2 crystallographic software package except for refinement, which was performed using SHELXL.[28] The CIF data were confirmed using the checkCIF/PLATON service. Supplementary crystallographic data for this study can be obtained free of charge from the Cambridge Crystallographic Data Centre at www.ccdc.cam.ac.uk/data_request/cif (CCDC-2370098 for **[Eu(hfa)$_3$(dpa)]$_n$**).

Acknowledgements

This work was supported by JSPS KAKENHI, Grant Numbers JP23K17925 and JP23K23420.

Keywords: MOFs · lanthanides · luminescence · helical structures · carbon dioxide

[1] H. Arakawa, M. Aresta, J. N. Armor, M. A. Barteau, E. J. Beckman, A. T. Bell, J. E. Bercaw, C. Creutz, E. Dinjus, D. A. Dixon, K. Domen, D. L. DuBois, J. Eckert, E. Fujita, D. H. Gibson, W. A. Goddard, D. W. Goodman, J. Keller, G. J. Kubas, H. H. Kung, J. E. Lyons, L. E. Manzer, T. J. Marks, K. Morokuma, K. M. Nicholas, R. Periana, L. Que, J. Rostrup-Nielson, W. M. H. Sachtler, L. D. Schmidt, A. Sen, G. A. Somorjai, P. C. Stair, B. R. Stults, W. Tumas, *Chem. Rev.* **2001**, *101*, 953–996.

[2] M. Aresta, A. Dibenedetto, A. Angelini, *Chem. Rev.* **2014**, *114*, 1709–1742.

[3] M. He, Y. Sun, B. Han, *Angew. Chem. Int. Ed.* **2013**, *52*, 9620–9633.

[4] M. Ding, R. W. Flaig, H.-L. Jiang, O. M. Yaghi, *Chem. Soc. Rev.* **2019**, *48*, 2783–2828.

[5] Z. Sun, Y. Liao, S. Zhao, X. Zhang, Q. Liu, X. Shi, *J. Mater. Chem. A* **2022**, *10*, 5174–5211.

[6] D.-X. Xue, Q. Wang, J. Bai, *Coord. Chem. Rev.* **2019**, *378*, 2–16.

[7] S. Mubarak, D. Dhamodharan, P. N. P. Ghoderao, H.-S. Byun, *Coord. Chem. Rev.* **2022**, *471*, 214741.

[8] N. Yanai, K. Kitayama, Y. Hijikata, H. Sato, R. Matsuda, Y. Kubota, M. Takata, M. Mizuno, T. Uemura, S. Kitagawa, *Nat. Mater.* **2011**, *10*, 787–793.

[9] A. Das, D. M. D'Alessandro, *Dalton Trans.* **2016**, *45*, 6824–6829.

[10] K. Miyata, Y. Konno, T. Nakanishi, A. Kobayashi, M. Kato, K. Fushimi, Y. Hasegawa, *Angew. Chem. Int. Ed.* **2013**, *52*, 6413–6416.

[11] C. Piguet, G. Bernardinelli, G. Hopfgartner, *Chem. Rev.* **1997**, *97*, 2005–2062.

[12] C. Xu, Q. Guo, X. Wang, H. Hou, Y. Fan, *Cryst. Growth Des.* **2011**, *11*, 1869–1879.

[13] X.-L. Wang, N.-L. Chen, G.-C. Liu, H.-Y. Lin, J.-W. Zhang, *Inorg. Chim. Acta* **2014**, *421*, 473–480.

[14] E. Yashima, N. Ousaka, D. Taura, K. Shimomura, T. Ikai, K. Maeda, *Chem. Rev.* **2016**, *116*, 13752–13990.

[15] P. M. Bhatt, Y. Belmabkhout, A. Cadiau, K. Adil, O. Shekhah, A. Shkurenko, L. J. Barbour, M. Eddaoudi, *J. Am. Chem. Soc.* **2016**, *138*, 9301–9307.

[16] A. Ebadi Amooghin, H. Sanaeepur, R. Luque, H. Garcia, B. Chen, *Chem. Soc. Rev.* **2022**, *51*, 7427–7508.

[17] T. Harada, Y. Nakano, M. Fujiki, M. Naito, T. Kawai and Y. Hasegawa, *Inorg. Chem.*, **2009**, *48*, 11242– 11250.

[18] D. Casanova, M. Llunell, P. Alemany and S. Alvarez, *Chem. Eur. J.*, **2005**, *11*, 1479–1494.

[19] B. Ugale, S. S. Dhankhar, C. M. Nagaraja, *Cryst. Growth Des.* **2018**, *18*, 2432–2440.

[20] M. H. V. Werts, R. T. F. Jukes, J. W. Verhoeven, *Phys. Chem. Chem. Phys.* **2002**, *4*, 1542–1548.

[21] Y. Kitagawa, R. Moriake, T. Akama, K. Saito, K. Aikawa, S. Shoji, K. Fushimi, M. Kobayashi, T. Taketsugu, Y. Hasegawa, *ChemPlusChem* **2022**, *87*, e202200151.

[22] G. Neurauter, I. Klimant, O. S. Wolfbeis, *Anal. Chim. Acta* **1999**, *382*, 67–75.

[23] C. W. Seifert, A. Paniagua, G. A. White, L. Cai, G. Li, *Eur. J. Org. Chem.* **2016**, *2016*, 1714–1719.

[24] M. Yamamoto, T. Nakanishi, Y. Kitagawa, K. Fushimi, Y. Hasegawa, *Mater. Lett.* **2016**, *167*, 183–187.

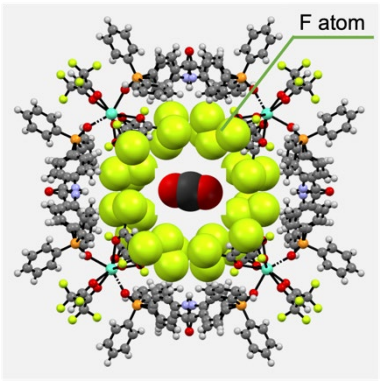
[25] M. Yamamoto, Y. Kitagawa, T. Nakanishi, K. Fushimi, Y. Hasegawa, *Chem. Eur. J.* **2018**, *24*, 17719–17726.

[26] T. Koizuka, K. Yanagisawa, Y. Hirai, Y. Kitagawa, T. Nakanishi, K. Fushimi, Y. Hasegawa, *Inorg. Chem.* **2018**, *57*, 7097–7103.

[27] G. M. Sheldrick, *Acta Crystallogr.* **2008**, *64*, 112–122.

[28] O. V. Dolomanov, L. J. Bourhis, R. J. Gildea, J. A. K. Howard, H. Puschmann, *J. Appl, Crystallogr.* **2009**, *42*, 339–341.

Entry for the Table of Contents



Novel lanthanide MOFs with CO_2 gas adsorption are demonstrated. The MOFs constructed cylindrical structure. The inner channel of cylindrical structure was covered fluorine atoms. The fluorine atoms enhance interaction with CO_2 gas molecules. Eu/Tb-mixed MOFs exhibited the change of ratiometric emission intensity between Eu and Tb by CO_2 gas adsorption behavior.